

April 24, 2019  
hep-ph/yymmdd

# Constraining top squark in R-parity violating $SUSY$ model using existing Tevatron data.

Subhendu Chakrabarti, Monoranjan Guchait and N. K. Mondal

*Department of High Energy Physics  
Tata Institute of Fundamental Research  
Homi Bhabha Road, Bombay-400005, India.*

## Abstract

Signal of lighter top squark has been looked for using Tevatron data in the di-electron plus di-jet channel. We find that the mass of the lighter top squark when it decays dominantly in the electron plus jet channel, can be ruled out up to 220 GeV at 95% C.L. using di-electron data. In the framework of R-parity breaking SUSY model we exclude relevant R-parity violating couplings for a range of top squark masses and other SUSY parameters. The bounds on R-parity violating couplings are very stringent for the parameter space where lighter top squark turns out to be the next to lightest supersymmetric particle.

# I. Introduction

The Minimal Supersymmetric Standard model(MSSM) [1] so far is one of the most credible candidate for the beyond standard model(SM) physics. There is no single evidence of supersymmetric (SUSY) particles, however, no observation can rule it out either. Therefore, hunting for SUSY in the next generation of colliders at Fermilab and at LHC experiments is a very challenging programme. At present, from the non observation of SUSY signals in the past experiments, mainly at LEP [2] and Tevatron [3], masses of SUSY particles have been constrained.

In MSSM, there is a mixing between the scalar superpartners of the two chirality states of fermions,  $\tilde{f}_L$  and  $\tilde{f}_R$ . The extent of mixing of these two chiral states is controlled by the off diagonal term  $m_f(A_f - \mu \tan \beta)$  in the sfermion mass matrix. It is obvious that the sfermions which are superpartners of the massive fermions will have larger mixing effect because of the explicit dependence on the corresponding fermion mass  $m_f$  i.e. sfermions of third generation receive a large splitting between two mass eigen states. Thus the two chirality states of top squarks  $\tilde{t}_L, \tilde{t}_R$ , has large mixing, resulting in large splitting between the two physical mass states  $\tilde{t}_1, \tilde{t}_2$  (assume  $m_{\tilde{t}_1} \lesssim m_{\tilde{t}_2}$ ) [4]. Moreover, because of the large Yukawa coupling, the soft SUSY masses ( $m_{\tilde{t}_L}, m_{\tilde{t}_R}$ ) also receive a large correction via the renormalisation group equation [5] which can push the lighter mass eigenstates,  $\tilde{t}_1$ , even below the top quark mass. Consequently, in a certain region of SUSY parameter space it may turn out to be the next to lightest SUSY particle(NLSP), the lightest neutralino  $\tilde{\chi}_1^0$  being the lightest SUSY particle (LSP). It is to be noted that in the canonical SUSY searches at colliders the missing energy due to the presence of  $\tilde{\chi}_1^0$  which is assumed to be stable and non interacting, plays a very crucial role [5].

In hadron colliders  $\tilde{t}_1$  can be produced copiously, since it is colored and comparatively lighter than the other sparticles. Therefore, in the context of SUSY searches at hadron colliders, top squark searches has received a special attention. The search strategy of top squark depend very crucially on its decay pattern. As for example, the loop induced flavour changing neutral current decay mode [6],

$$\tilde{t}_1 \rightarrow c \tilde{\chi}_1^0 \quad (1)$$

yields acoplanar jets and missing energy from top squark pair production. At Tevatron, data corresponding to RUN-I experiment has been analysed to find top squark signal in this channel. Negative results have constrained lighter top squark mass,  $m_{\tilde{t}_1} \gtrsim 119$  GeV (102 GeV) for  $m_{\tilde{\chi}_1^0} = 40(50)$  GeV [7]. However, if kinematically accessible, the top squark decays dominantly into a lighter chargino ( $m_{\tilde{\chi}_1^\pm}$ ) and b quark,

$$\tilde{t}_1 \rightarrow b + \tilde{\chi}_1^+ . \quad (2)$$

Because of the cascade decays of  $\tilde{\chi}_1^\pm$  into neutralino and massless fermions,  $\tilde{\chi}_1^\pm \rightarrow \tilde{\chi}_1^0 f \bar{f}'$ , the top squark pair production leads final states consisting leptons and jets accompanying by missing transverse energy [8]. Beside these popular decay modes eq.1 and 2, there are also

other interesting decay channels which yield a variety of signals in the colliders. All those decay modes will be discussed in the next section.

It is found that top squark mass upto  $\sim 170$  GeV can be probed in RUN-II experiment at Tevatron with integrated luminosity  $2 \text{ fb}^{-1}$  per experiments for the entire region of SUSY parameter space where  $\tilde{t}_1$  state appears to be NLSP [9] leading the decay mode (eq.1) with 100% branching ratio. For the scenario, when  $m_{\tilde{t}_1}$  is heavier than lighter chargino mass,  $4 \text{ fb}^{-1}$  luminosity is required for the same discovery limit in the dilepton plus missing energy channel which is heavily contaminated by top backgrounds. The upgraded RUN-II experiment which may deliver high luminosity  $\sim 20 \text{ fb}^{-1}$  may extend this reach upto  $\sim 220$  GeV [9].

However, top squark phenomenology shows up new features in the framework of R-parity violating(RPV) SUSY models. In the SUSY models R-parity conservation(RPC) is assumed to forbid the decay of proton ensuring conservation of lepton and baryon numbers, L and B respectively. However, one can avoid proton decay problem by invoking either L or B conservation. Thus one can have two kind of RPV SUSY models corresponding to L or B violation. As a consequence, in any SUSY cascade decay process within the framework of RPV SUSY model, the LSP can have decay modes either in the leptonic or hadronic channels leading multileptons and multijets in the final states with or without missing energy. The prospects of SUSY searches at Tevatron in the context of R-parity breaking SUSY model has been investigated in great detail [10].

In RPV SUSY model, the superpotential is

$$W = W_{MSSM} + W_{R_p}, \quad (3)$$

where  $W_{MSSM}$  is the superpotential containing yukawa type of interactions giving masses to the fermions and  $W_{R_p}$  corresponds to the potential containing terms which violate L and B numbers,

$$W_{R_p} = \lambda_{ijk} L_i L_j E_K + \lambda'_{ijk} L_i Q_j D_k + \lambda''_{ijk} U_i D_j D_k + \mu_i L_i H_2. \quad (4)$$

Here  $i, j, k$  are the generation indices,  $\lambda$ ,  $\lambda'$  and  $\lambda''$  are the dimensionless yukawa couplings. The superfields L, Q represent the SU(2) doublets for leptons and quarks respectively where as singlets U, D and E stand for up type, down type quarks and charged leptons respectively. Last term in eq. 4 mixes the mass terms of the lepton and higgs doublets [11]. However, in the present case we will work in the context of spontaneous [12] RPV neglecting this bi-linear term in eq. 4.

In this work we focussed on the top squark decays in RPV SUSY model. Considering only lepton number violation the  $\lambda'_{ij3}$  coupling which leads to a new decay channel of  $\tilde{t}_1$ ,

$$\tilde{t}_1 \rightarrow l + q. \quad (5)$$

As a consequence, in this scenario the pair of top squark production are signalled by dilepton plus di-jets. As we know, the identical final states also appear due to the pair production

of Leptoquark( $LQ$ ) assumed to be the composite object of lepton and hadron [13] and its subsequent decays into the corresponding lepton and quark

$$LQ \rightarrow \ell + q. \quad (6)$$

At Tevatron experiments, the searches for all three generations of  $LQ$  which are signalled by  $ee + 2\text{jets}$ ,  $\mu\mu + 2\text{ jets}$  and  $\tau\tau + 2\text{ jets}$  respectively were carried out [14, 15, 16]. This remarkable similarity between the final states due to the pair production of top squarks in RPV SUSY scenario and Leptoquark pair production and its subsequent decays via eq.6 motivated us to exploit the existing data corresponding to this Leptoquark searches to constrain top squark mass which is involved in the production mechanism. Recall that  $\tilde{t}_1$  states has also other RPC decay modes as well which will be discussed in the next section. The branching ratio(BR) of  $\tilde{t}_1$  in the RPV channel, eq.5, is controlled by RPV couplings and as well as other SUSY parameters which are involved in determining the decay rates corresponding to RPC decay channels. In this work our main goal is to analyse top squark signal in the di-electron plus di-jet channel and compare it with the data corresponding to this final state which was used for 1st the generation of Leptoquark search at Tevatron. This leads to lower limit of top squark mass for a given BR of top squark in the RPV channel. Moreover, the RPV couplings( $\lambda'_{13j}$ ) can be excluded for a given top squark mass and SUSY parameter space. In the case of dimuon channel, we found in the paper of Ref [16] that the background corresponding to this channel has been analysed using neural network (NN) analysis and the same NN has been trained to analyse signal. Because of this we could not perform the analysis for this channel, while the investigation of the ditau channel due to the  $\lambda'_{33j}$  RPV coupling is now under progress. Hereafter, whenever we will refer to data, that will correspond to the data in the di-electron plus di-jet channel.

It may be recalled that these RPV decay channels drawn a lot of attention for the possible interpretation to explain the excess of high  $Q^2$  events reported in H1 and ZEUS experiments few years back [18]. In that context, implications of these channels was examined at Tevatron [19].

It is worth mentioning here the existing bounds of the RPV couplings which are relevant for the present purpose. From the direct production of  $\tilde{t}_1$  in electron-proton collision at HERA, the H1 experiment predicts a bound,  $\lambda'_{131} \lesssim 0.05(.02)$  at 95% C.L for  $m_{\tilde{t}_1}=200(100)$  GeV [20]. A bound on  $\lambda'_{131}$  also exist from atomic parity violation(APV),  $\lambda'_{131} \lesssim 0.07$  at 95% C.L for  $m_{\tilde{t}_1}=200$  GeV [21]. The forward-backward asymmetry in  $e^+e^-$  collision predicts the bound on  $\lambda'_{132} \lesssim 0.28$  for  $m_{\tilde{t}_L}=100$  GeV [22]. The stringent bound on  $\lambda'_{133}$  comes from neutrino data. In the framework of RPV SUSY model the neutrino masses can be generated from the tree level contributions due to the bi-linear terms or loop contributions from the trilinear  $\lambda$  and  $\lambda'$  couplings [23]. The detailed phenomenological analysis has been done using neutrino data including trilinear and bi-linear couplings [24, 25]. The most favoured large mixing angle solution constraints the trilinear couplings  $\lambda'_{133} \lesssim 10^{-4}$  assuming  $M_{susy} = 100$  GeV [25].

We have organised our paper as follows. In section II, we discuss branching ratios of top squark decay into various channels in the context of RPV SUSY model. Our analysis

is described in section III followed by our results in section IV. Finally we conclude with a summary in section V.

## II. Top squark decay in R-parity violating SUSY model

As mentioned in the last section that the lighter state of top squark,  $\tilde{t}_1$ , has many phenomenologically interesting decay modes depending on its mass. The most dominant decay mode of  $\tilde{t}_1$ , if kinematically accessible, is via lighter chargino state,  $\tilde{\chi}_1^\pm$  and  $b$  quark, (eq.2). In the absence of this two body charged current decay mode, the flavour changing neutral current decay mode and the four body decay channel, into a  $b$  quark, the LSP( $\tilde{\chi}_1^0$ ) and two approximately massless fermions [26, 27],

$$\tilde{t}_1 \rightarrow b\tilde{\chi}_1^0 f \bar{f}' \quad (7)$$

are the only available decay modes and very competitive to each other. This 4-body decay channel occurs via many diagrams involving a variety of heavier SUSY particles in the intermediate state. In the papers of ref. [26, 27], the decay pattern in this channel has been discussed elaborately over a wide range of SUSY parameter space assuming R-parity conservation. Surprisingly, in certain region of SUSY parameter space the 4-body decay mode takes over the loop level decay mode and the branching ratio may shoot up to  $\sim 100\%$ . It implies that the signal corresponding to the neutral current decay modes of top squarks will be suppressed. The impact of this 4 body decay modes in the context of top squark searches at upgraded Tevatron has been discussed [28, 29]. Beside these decay channels of  $\tilde{t}_1$ , there are also a few other decay modes which may be interesting from the phenomenological point of view. As for example, if kinematically accessible, the three body decay mode to bottom quark and a  $W$  boson or a charged Higgs scalar  $H^\pm$ , and a neutralinos,  $\tilde{t}_1 \rightarrow bW^\pm \tilde{\chi}_1^0$  or  $\tilde{t}_1 \rightarrow bH^\pm \tilde{\chi}_1^0$  may open up [30]. Moreover, in the light slepton scenario which is viable in some SUGRA models [31]  $\tilde{t}_1$  decays via the final states containing sleptons,  $\tilde{t}_1 \rightarrow b\tilde{\ell}\nu, b\tilde{\ell}'\nu$  [32].

In RPV SUSY model, top squark decay channel, eq. 5 opens up due to the interaction

$$\lambda'_{i3j} \ell_i \tilde{t}_L q_j + h.c \quad (8)$$

which is a subset of the Lagrangian given by eq.4. The species of the lepton and quark depend on the choice of  $i$  and  $j$  respectively, where  $i, j=1,2,3$ . Since we are not restricted to the jet flavour therefore  $j$  can be of anything 1-3 in the decay process, eq. 5.

Neglecting the fermion masses, the decay width of  $\tilde{t}_1$  in the RPV channel (eq. 5) is given by

$$\Gamma_R(\tilde{t}_1 \rightarrow \ell + q) = \frac{\lambda'^2_{i3j} \cos^2 \theta_{\tilde{t}}}{16\pi} m_{\tilde{t}_1}^2 \quad (9)$$

$\theta_{\tilde{t}}$  is the mixing angle in the top squark sector; it appears due to the replacements of  $\tilde{t}_L$  by the physical states  $\tilde{t}_1$ . The BR in this channel is given by,

$$\epsilon = \frac{\Gamma_R(\tilde{t}_1 \rightarrow l + q)}{\Gamma_R(\tilde{t}_1 \rightarrow l + q) + \Gamma(\tilde{t}_1 \rightarrow RPC)} \quad (10)$$

where  $\Gamma(\tilde{t}_1 \rightarrow RPC)$  stands collectively for the total decay width in all accessible RPC decay modes of  $\tilde{t}_1$  states. The rate of those RPC decay modes depend on SUSY parameters, particularly on the SU(2) gaugino mass  $M_2$  (assuming electroweak gaugino mass relation,  $M_1 \simeq \frac{M_2}{2}$ , where  $M_1$  is the U(1) gaugino mass), the higgsino mass parameter  $\mu$  and  $\tan \beta$  - the ratio of the vacuum expectation values of two higgs doublets which give up type and down type quark masses. Beside these parameters, it involves other sparticle masses and parameters, e.g. mass of sleptons ( $m_{\tilde{\ell}}$ ), mass of squarks ( $m_{\tilde{q}}$ ) and A-terms, the trilinear couplings. We investigate the relative rates of the RPV decay mode over the RPC decay modes for a wide range of SUSY parameter space.

In fig.1, we present contour plots for the constant BR ( $\epsilon$ ) corresponding to the RPV decay modes of  $\tilde{t}_1$  in the  $m_{\tilde{t}_1} - \lambda'_{i3j}$  plane for a fixed set of SUSY parameters:  $M_2 = 125$  GeV,  $\mu = 400$  GeV,  $\tan \beta = 4$ ,  $m_{\tilde{q}} = 300$  GeV and  $m_{\tilde{\ell}} = 200$  GeV and  $\cos \theta_{\tilde{t}} = 0.8$ . We find for low  $m_{\tilde{t}_1}$ , where the two body chargino decay mode (eq.2) is kinematically inaccessible the RPV decay modes has comparatively appreciable rates even for very small value of  $\lambda'_{i3j} (\sim 10^{-4})$ . In contrast, for higher  $\tilde{t}_1$  masses, the two body charged current decay mode will open up resulting in the suppression of the RPV decay. In this case the RPV mode will be important for  $\lambda'_{i3j} \sim O(0.1)$ .

### III. Squark production: Event Analysis

At Tevatron top squark pairs are produced via quark-antiquark annihilation and gluon gluon fusion,

$$q\bar{q}, gg \rightarrow \tilde{t}_1 \tilde{t}_1^*. \quad (11)$$

Since, this pair production mechanism is dominated by the QCD process, the cross section depends solely on  $m_{\tilde{t}_1}$  [33]. The SUSY-QCD corrections enhance the cross section by another  $\sim 30\%$  over most of the SUSY parameter space [34]. We estimate the cross section setting renormalisation and factorisation scale at  $Q^2 = \hat{s}$  and use CTEQ3L [35] for the parton distribution functions. The typical top squark pair production cross section ranges from  $\sim 10$ .-0.1 pb for  $m_{\tilde{t}_1} \sim 100$ -200 GeV at  $\sqrt{s} = 1.8$  TeV.

We analyse the top squark pair production in the di-electron plus di-jet channel which originates because of the top squark decay via eq. 5. As we discussed earlier that the same type of event topology also appears due to the pair production of 1st generation of Leptoquark and its subsequent decay through eq. 6. The dominant SM backgrounds corresponding to this signal come from Drell-Yan process. The other sources of backgrounds are due to the production of  $WW$ ,  $W$ +jets,  $t\bar{t}$  and  $Z$ +jets followed by the leptonic decay of vector boson. For the present purpose we do not estimate the cross sections for each of these background processes. Instead we closely follow the analysis as described in the paper [15] for 1st generation of Leptoquark searches at D0 experiment, where the kinematic cuts are chosen to effectively suppress these backgrounds.

The number of signal events for a given  $m_{\tilde{t}_1}$  is given by,

$$n_{sig} = \sigma_{\tilde{t}_1\tilde{t}_1^*} \cdot \epsilon_d \cdot \mathcal{L} \cdot \epsilon \quad (12)$$

Here,  $\epsilon_d$  stands for the detection efficiency which includes the acceptance efficiency due to the selection and as well as background rejection cuts and all systematic efficiencies like trigger and lepton identification efficiencies. The luminosity for the given set of data is given by  $\mathcal{L}$  and  $\sigma_{\tilde{t}_1\tilde{t}_1^*}$  represents the top squark pair production cross section and  $\epsilon$  is the BR of  $\tilde{t}_1$  decay into lepton plus jet. We generate events using PYTHIA(V6.206) [36] producing top squark pair, which are allowed to decay via the eq. 5. We take into account the effect of initial and final state radiation as well as fragmentation effects in the event generation. We adopt the following strategy to compute the signal cross section for a given  $m_{\tilde{t}_1}$  and then comparing our results with the existing data we obtain limits of  $m_{\tilde{t}_1}$  and RPV couplings.

- First, for a given  $m_{\tilde{t}_1}$ , we compute acceptance efficiency for the signal process by generating events using PYTHIA [36] applying the same set of cuts which are used in the analysis for the first generation of Leptoquark searches [15]. Then we multiply the respective systematic efficiencies, e.g. trigger and lepton identification efficiencies appropriately with the acceptance efficiency to obtain overall detection efficiency  $\epsilon_d$ .

- Secondly, from the existing data corresponding to this final state, for a given  $\epsilon$  and  $m_{\tilde{t}_1}$ , we estimate the cross section limit using eq.12 following Bayesian approach with a flat prior probability distribution of cross section. The systematic and statistical uncertainties are included taking Gaussian prior distribution of each of them. Then the limit of cross section is compared with the theoretical prediction for a given  $m_{\tilde{t}_1}$  setting a fixed value of  $\epsilon$ .

- And finally, repeating this procedure for various  $m_{\tilde{t}_1}$ , the upper limit of  $\epsilon$  can be obtained for each  $m_{\tilde{t}_1}$ . Eventually, this upper limit of  $\epsilon$  can be translated to obtain upper bound of RPV coupling for a given set of SUSY parameters.

Now, in the following we discuss event analysis for the di-electron plus di-jet channel.

The pair production of top squark and subsequent decays of each top squarks in the RPV channel via coupling  $\lambda'_{13j}$

$$\tilde{t}_1\tilde{t}_1^* \rightarrow ee + qq \quad (13)$$

results the final states,  $e e + 2$  jets. As discussed earlier that it is identical to the final states due to the pair production of 1st generation of  $LQ$  and its subsequent decay via eq. 6. For our signal Monte Carlo, we followed the analysis very closely as described in Ref. [15] where search for 1st generation  $LQ$  with same final states has been described and then compare our results with the data. As we mentioned above that the dominant SM backgrounds corresponding to this di-electron final state are from Drell-Yan production with two or more jets,  $t\bar{t}$  production and multijet events in which two jets are miss identified as electrons<sup>1</sup>. In our simulation we selected events in the hadronic and electromagnetic calorimeter cells in pseudorapidity and azimuthal angle( $\phi$ ) of size  $\Delta\eta \times \Delta\phi = 0.1 \times 0.1$ . Cells with  $E_T > 1$  GeV

---

<sup>1</sup>The probability of faking a jet as electron is very small  $\sim O(10^{-3})$  [15]

are taken as initial seeds to form calorimetric tower. For the jet reconstruction we use the routine PYCELL in PYTHIA [36]. Jets are reconstructed with cone radius 0.7 and accepted only those which has transverse energy  $E_T > 8$  GeV and are smeared by  $0.5 \times \sqrt{E_T}$ . Events are subjected to the following sets of cuts mentioned in the paper of Ref. [15] ,

1. Two electrons with  $E_T^e > 20$  GeV and within the coverage for central calorimeter(CC)  $|\eta| < 1.1$  and for endcap calorimeter (EC)  $1.5 < |\eta| < 2.5$ .
2. At least two jets having  $E_T^j > 15$  GeV and  $|\eta| < 2.5$ .
3. Isolation between electrons and jets are maintained by requiring  $\Delta R_{ej} > 0.7$  where  $\Delta R = \sqrt{\Delta\phi^2 + \Delta\eta^2}$
4. Events of having di-electron invariant mass between  $82 < M_{ee} < 100$  GeV are rejected.
5. The total visible transverse energy( $S_T$ ) satisfy the cut  $S_T > 350$  GeV where  $S_T = H_T^e + H_T^j$ ,  $H_T^e$  = sum of the  $E_T$  of the two electrons;  $H_T$ =sum of the  $E_T$  of all jets.

The cuts 1-3 are the event selection cuts where as cut 4-5 are the background rejection cuts. The cut 4 is used to avoid the contamination due to the events from Z production. In the Drell Yan process, leptons and jets are not so hard as in the case of signal process for  $m_{\tilde{t}_1} \sim 100$ -200 GeV. So a cut on the sum of the transverse energies of visible particles in the final state drastically reduce this background. The cut 5 serves that purpose and brings down the level of background to a negligible level. We found that the signal acceptance efficiencies which is only due to the kinematic cut effect vary from 0.1 - 15% for  $m_{\tilde{t}_1} = 80$ -200 GeV. We take into account the electron identification efficiencies which are  $74 \pm 3\%$ ,  $66 \pm 4\%$  and  $68 \pm 9\%$  for CC-CC, CC-EC and EC-EC regions respectively [15] by multiplying appropriately with the acceptance efficiencies which are obtained from PYTHIA, and we refer this as a detection efficiency. In table.1, we show the detection efficiencies folding all other systematic efficiencies together for various choices of  $m_{\tilde{t}_1}$ . For a given  $m_{\tilde{t}_1}$ , we can obtain from the knowledge of detection efficiency the number of di-electron events for a given  $\epsilon$  and luminosity. The total integrated luminosity is  $123 \pm 7.0$  pb $^{-1}$  for this di-electron data set [15].

In the paper of Ref. [15] it is reported that no signal events exist in this di-electron channel where as the number of background events after applying all sets of cuts as described above is  $0.44 \pm 0.06$  [15]. The uncertainty in background estimation is mainly due to the systematics. We exploit this information to obtain the limits of top squark pair production cross sections at 95% C.L using Bayesian method for different choices of  $m_{\tilde{t}_1}$  and for a given value of  $\epsilon$ . In this cross section limit calculation we take into account the uncertainties in background estimation, in the luminosity measurements and the uncertainty in detection efficiency.

Following the strategy as outlined above, using the data which implies that no signal events with a background  $0.44 \pm 0.06$ , we obtain limits of top squark pair production cross sections at 95% C.L. for two choices of  $\epsilon = 0.5$  and 1. In fig.2 we show these limits (solid lines)



along with the theoretical predictions(dashed line). In theoretical calculation we multiply the K-factor 1.3 with the Born level cross section to take into account the next to leading order effect [34]. Notice that, one can rule out top squark mass upto 220(165) GeV for the choice of  $\epsilon=1(0.5)$  in a model independent way. Moreover, as we explained already that the upper limits of cross sections which are consistent with di-electron data predict upper limits of  $\epsilon$  for a given  $m_{\tilde{t}_1}$ . In fig.3, we present these upper limits of  $\epsilon$  for each value of  $m_{\tilde{t}_1}$  which is ruled out by data at 95% C.L. In the context of RPV SUSY model this upper limit of  $\epsilon$  can be translated to obtain an upper limit of respective RPV couplings for a given  $m_{\tilde{t}_1}$  and SUSY parameter space. In fig.4 we show the excluded region in the  $\lambda'_{13j} - m_{\tilde{t}_1}$  plane for a given set of SUSY parameters and for two choices of  $\tan\beta=5$  and 30. In each figure we excluded region for two extreme values of  $\cos\theta_{\tilde{t}}=0.02$  and 0.95. The choice of our SUSY parameters for fig.3 and 4 are(units are in GeV):

$$\begin{aligned}
M_2 &= 130, \quad \mu = 500, \quad \tan\beta = 5(30). \\
m_{\tilde{\chi}_1^\pm} &= 515(514), \quad m_{\tilde{\chi}_2^\pm} = 121(126), \\
m_{\tilde{\chi}_1^0} &= 63(65), \quad m_{\tilde{\chi}_2^0} = 122(126) \\
m_{\tilde{\chi}_3^0} &= 504(506) \quad m_{\tilde{\chi}_4^0} = 515(511) \\
m_{\tilde{q}} &= 300, \quad m_{\tilde{\ell}} = 200, \quad A_{b,\tau,t} = 200
\end{aligned} \tag{14}$$

We discuss results in the next section.

## IV. Results and Discussion

We have computed the signal cross section in the di-electron plus di-jet channel due to the top squark pair production at Tevatron in the framework of RPV SUSY model. In addition to the RPC decay modes,  $\tilde{t}_1$  also decays via two body decay channel into lepton and quark due to the presence of RPV couplings. The relative rates of this RPV decay mode are shown in fig.1 as contours of fixed value of its BR  $\epsilon$  in the  $\lambda'_{13j} - m_{\tilde{t}_1}$  plane for a given set of SUSY parameter space. In the lower region of  $m_{\tilde{t}_1}$  values, in addition to the RPV decay mode (eq. 5) other available RPC decay modes are the loop induced decay channel, (eq. 1) and 4-body decay mode, (eq. 7) which are of the same order in perturbation theory i.e  $\mathcal{O}(\alpha^3)$ . In this mass region as expected, the RPV decay mode will dominate over the other decay modes for most of the parameter space depending on the value of  $\lambda'_{13j}$  and  $\cos\theta_{\tilde{t}}$ . Therefore, in this region of  $m_{\tilde{t}_1}$ , even very small value ( $\sim 10^{-4}$ ) of  $\lambda'_{13j}$  coupling will yield appreciable rates for RPV decay suppressing the two RPC decay modes. Once the value of  $m_{\tilde{t}_1}$  crosses the  $m_{\tilde{\chi}_1^\pm}(=112 \text{ GeV})$  threshold, the two body charged current decay mode (eq.2) opens up, which is very much competitive to the RPV decay mode. As a result, large value of RPV coupling  $\lambda'_{13j}(\sim 0.1)$  is needed to make the RPV decay mode comparable with the two body charged current decay mode for a given  $m_{\tilde{t}_1}$ . We present this result in fig.1 for a single

SUSY parameter point. However, we have checked that this pattern more or less exists for an entire region of SUSY parameter space which are accessible at Tevatron. We intend to emphasise that once the two body charged current decay mode of  $\tilde{t}_1$  opens up then it becomes dominant, otherwise the RPV decay mode is the most dominant one in comparison to the loop level and 4-body decay modes.

In fig.2 we present the limiting values of signal cross section at 95% C.L for two values of  $\epsilon$  ( $= 1$  and  $0.5$ ). We also show the theoretical prediction of top squark pair production cross section including K-factor [34] by the dashed line in the same plane. Comparing the cross section limits with the theoretical predictions top squark masses can be constrained as a function of  $\epsilon$ . For instance, from the di-electron plus di-jet data we set the limit of top squark mass,  $m_{\tilde{t}_1} \gtrsim 220(165)$  GeV for  $\epsilon=1(0.5)$ . Notice that the limit of  $m_{\tilde{t}_1}$  depends very strongly on  $\epsilon$ . However, there is a 10-20% theoretical uncertainty due to the choice of renormalisation and factorisation scales and parton distribution functions in cross section calculations. Note that these limits on  $m_{\tilde{t}_1}$  are obtained in a model independent way.

In fig.3, we show the upper limits of top squark decay  $\text{BR}(\epsilon)$  at 95% C.L for various  $m_{\tilde{t}_1}$  values. These upper limits do not depend on any specific models. More precisely, if  $\tilde{t}_1$  state has the decay channel as eq. 5 then the corresponding BR is restricted by existing data, as shown in fig.3. As for example, for  $m_{\tilde{t}_1}=100$  GeV, the 95% C.L. upper limit on  $\epsilon$  is 0.35.

In the framework of RPV SUSY model the decay rate of  $\tilde{t}_1$  is mainly controlled by  $\lambda'_{13j}$  for a given  $m_{\tilde{t}_1}$  and  $\cos\theta_{\tilde{t}}$  (see eq. 5). Therefore, in this model, the upper limit of  $\epsilon$  can be translated to the upper limit of  $\lambda'_{13j}$  for a fixed  $m_{\tilde{t}_1}$  and other SUSY parameters which determine the decay rates of  $\tilde{t}_1$  into the RPC decay modes (see eq. 10). In fig.4, at 95% C.L, we show the exclusion region in the  $\lambda'_{13j} - m_{\tilde{t}_1}$  plane using data. The set of SUSY parameters corresponding to this plot is given by eq. 14. Notice that for a lower range of  $m_{\tilde{t}_1}$  ( $\sim 100$  GeV) where it appears to be NLSP, the RPV couplings are restricted to be  $\lambda'_{13j} \lesssim 10^{-4}(10^{-3})$ . Note that in this region for lower value of  $\cos\theta_{\tilde{t}}=0.02$ , the RPV decay rate is suppressed (see eq. 5) leading to weaker bounds where as for higher values of  $\cos\theta_{\tilde{t}}$ , bounds are turn out to be relatively better. However, the limits also become comparatively weaker in the higher side of  $m_{\tilde{t}_1}$  where it is heavier than  $m_{\tilde{\chi}_1^\pm}$ . This is because, when the two body charged current decay mode of  $\tilde{t}_1$  (eq. 2) opens up, then it becomes very competitive with the RPV decay mode leading lower BR for the RPV channel. Consequently, in this region, the BR limit constrains only higher side of  $\lambda'_{13j}$  for a given  $m_{\tilde{t}_1}$ .

It is obvious from eq. 5, that the higher values of  $\cos\theta_{\tilde{t}}$  will yield more stronger limits on  $\lambda'_{13j}$ . With the increase of  $\tan\beta$ , the two body loop decay and 4-body decay [26, 27] widths enhances as the virtuality between  $m_{\tilde{t}_1}$  and  $m_{\tilde{\chi}_{1,2}}$  decreases resulting a suppression of  $\epsilon$  for a given  $m_{\tilde{t}_1}$ , which eventually leads a less constrained region in the  $\lambda'_{13j} - m_{\tilde{t}_1}$  plane. It is clear that for the region of  $m_{\tilde{t}_1} \gtrsim m_{\tilde{\chi}_1^\pm}$  i.e when  $\tilde{t}_1$  is not NLSP, the bounds on RPV couplings are comparatively weaker.

## V. Summary

We investigate the di-electron plus di-jet signal due to the top squark pair production at Tevatron. Identical final states also appear due to the first generation of Leptoquark production. Exploiting the existing experimental data analysed by D0 group at Tevatron in the context of Leptoquark searches we try to constrain the top squark mass for various values of BR of top squarks in the RPV channel. Using D0 data and assuming the BR of  $\tilde{t}_1$  decay via the eq. 5,  $\epsilon=1(0.5)$  we predict lower limits on  $m_{\tilde{t}_1} \gtrsim 220(165)$  GeV at 95% C.L. Repeating this exercise for various value of  $m_{\tilde{t}_1}$  we exclude part of the parameter space in the  $\epsilon - m_{\tilde{t}_1}$  plane as shown in fig.3 in a model independent way.

In the framework of RPV SUSY model, this exclusion region in  $\epsilon - m_{\tilde{t}_1}$  plane converted to a corresponding exclusion region in the  $\lambda'_{13j} - m_{\tilde{t}_1}$  plane as shown in fig.4 for a given set of SUSY parameter space. We exclude  $\lambda'_{13j} \lesssim 10^{-4}$  for  $m_{\tilde{t}_1} = 100$  GeV and  $\tan \beta = 5$  where as for high  $\tan \beta = 30$  region this limit turns out to be relatively weak,  $\lambda'_{13j} \lesssim 10^{-3}$ . Notice that when  $\tilde{t}_1$  state appears to be NLSP, the limits are very stringent and comparable to the limit, for the case  $\lambda'_{131}$ , obtained from neutrino data [25] as discussed in Sec.I. However, for,  $m_{\tilde{t}_1} \gtrsim m_{\tilde{\chi}_1^\pm}$ , the present analysis does not give any better limit than the others obtained from H1 experiments and APV measurements [20, 21] and also from neutrino data [25]. We conclude that our predicted bounds are very stringent in the region where  $\tilde{t}_1$  state appears to be NLSP.

## Acknowledgement:

The authors are grateful to D. P. Roy for useful discussions and reading of the manuscript. MG is thankful to Sunanda Banerjee and Amitava Datta for many helpful discussions.

## References

- [1] For reviews of the Supersymmetry, see e.g. H. E. Haber and G. Kane, Phys. Rep. 117 (1985) 75; M. Drees and S. Martin, CLTP Report (1995) and hep-ph/9504324.
- [2] ALEPH Collaboration, Phys. Lett. B469 (1999) 303; DELPHI Collaboration, Phys. Lett. B496 (2000) 59; L3 Collaboration, Phys. Lett. B471 (1999) 308; OPAL Collaboration, Phys. Lett. B456 (1999) 95; for a summary on stop searches at LEP, see: S. Rosier-Lees et al., hep-ph/9901246.
- [3] T. Affolder et. al, The CDF collaboration, hep-ex/0106001 and references therein.
- [4] J. Ellis and S. Rudaz, Phys. Lett. B128 (1983) 248; M. Drees and K. Hikasa, Phys. Lett. B252 (1990) 127.

- [5] For a review of mSUGRA and for the physics implications at the [Tevatron Run II, see: S. Abel et al., Report of the “SUGRA working group for “RUN-II at the Tevatron”, hep-ph/0003154 and references therein.
- [6] K.I. Hikasa and M. Kobayashi, Phys. Rev. D36 (1987) 724.
- [7] D0 Collaboration (S. Abachi et al.), Phys. Rev. Lett. 76 (1996) 2222; CDF Collaboration (T. Affolder et al.), Phys. Rev. Lett. 84 (2000) 5704; for a summary on stop searches at the Tevatron, see: A. Savoy-Navarro for the CDF and D0 Collaborations, Report FERMILAB-CONF-99-281-E (Nov. 1999).
- [8] H. Baer, J. Sender and X. Tata, Phys. Rev. D50 (1994) 4517.
- [9] R. Demina, J. Lykken, K. Matchev and A. Nomerotski, Phys. Rev. D62 (2000) 035011.
- [10] D. P. Roy, Phys. Lett B282 (1992) 270; H. Baer, C Kao and X. Tata, Phys. Rev. D51 (1995) 2180; M. Guchait and D. P. Roy, *ibid* D54 (1996)3276; Report of the working group for “Searching for R-parity violation at Run-II of Tevatron”, B. Allanach et. al., hep-ph/9906224.
- [11] Report of the Group R-parity Violation, R. Barbieri, et. al, hep-ph/9810232 and references therein.
- [12] C. S. Aulakh and R. N. Mahapatra, Phys. Lett. B119 (1983) 136; G. G. Ross and J. W. F. Valle, *ibid* B151 (1985) 375.
- [13] J. Pati and A. Salam, Phys. Rev. D10 (1974) 275; E. Eichten et. al. *ibid*, 34 (1986) 1547; W. Buchmuller and D. Wyler Phys. Lett. B177 (1986) 377; E. Eichten et.al. *ibid* Phys. ReV. Lett, 50 (1983) 811; H. Georgi and S. Glashow, Phys. ReV. Lett. 32 (1974) 438.
- [14] F. Abe et. al., CDF collaboration, Phys. Rev. Lett. 79 (1997) 4327.
- [15] V. M. Abazov et. al., D0 collaboration, Phys. Rev. D64 (2001) 092994.
- [16] B. Abbott et. al., D0 collaboration, Phys. Rev. Lett. 84 (2000) 2088.
- [17] S. Chakrabarti, M. Guchait and N. K. Mondal , in preparation
- [18] H1 collaboration, C. Adloff et .al Z. Phys. C74 (1997) 191; ZEUS collaboration, J. Breitweg et. al. *ibid* C74 (1997) 207.
- [19] M. Guchait and D. P. Roy, Phys. Rev. D57 (1998) 4453.
- [20] C. Adlof et. al. H1 collaboration, European Physics Journal C20, (2001) 639.
- [21] S. C. Bennet, C. E. Wieman, Phys. Rev. Lett. 82 (1999) 2484. C. S. Wood et. al. Science 275 (1997) 1759.

- [22] V. Barger, G. F. Giudice and T. Han, Phys. Rev. D40(1989) 2987.
- [23] A. Abada, G. Bhattacharya and M. Losada, Phys. Rev. D66 (2002) 071701(R) and references therein.
- [24] A. Abada and M. Losada, Nucl. Phys. B585 (2000) 45.
- [25] A. Abada and M. Losada, Phys. Lett. B492 (2000) 310.
- [26] C. Boehm, A. Djouadi and Y. Mambrini, Phys. Rev. D61 (2000) 095006.
- [27] A. Djouadi and Y. Mambrini, Phys. Rev. D63 (2001) 115005.
- [28] A. Djouadi, M. Guchait and Y. Mambrini, Phys. Rev. D64 (2001) 095014.
- [29] S. P. Das, A. Datta and M. Guchait, Phys. Rev. D65 (2002) 095006.
- [30] W. Porod and T. Wohrmann, Phys. Rev. D55 (1997) 02907.
- [31] See, e.g. L. E. Ibanez and G. G. Ross, Phys. Lett. B110, (1982) 215; L. E. Ibanez and J. Lopez, Nucl. Phys. B233 (1984) 511; M. Drees and M. M. Nojiri, Nucl. Phys. B369 (1992) 54; N. Polonosky and A. Pomarol, Phys. Rev. D51, (1995) 6532; Y. Kawamura, H. Murayama and M. Yamaguchi, Phys. Rev. D51 (1995) 1337.
- [32] A.K. Datta, M. Guchait and K.K. Jeong, Int. J. Mod. Phys. A14 (1999) 2239. W. Porod, Phys. Rev. D59 (1999) 095009.
- [33] G. Kane and J. P. Leveille, Phys. Lett. B112 (1982) 227; P. R. Harrison and C.H. Llewellyn-Smith, Nucl. Phys. B213 (1983) 223; C. Reya and D. P. Roy, Phys. Rev. D32 (1985) 645; S. Dawson, E. Eichten and C. Quigg, *ibid* 31 (1985) 1581; H. Baer and X. Tata, Phys. Lett. B160 (1985) 159.
- [34] W. Beenakker, M. Kramer, T. Plehn, M. Spira and P. M. Zerwas, Nucl. Phys. B515 (1998) 3.
- [35] CTEQ collaboration, H. L. Lai *et al*, Phys. Rev. D55 (1997) 1280.
- [36] T. Sjostrand, P. Eden, C. Friberg, L. Lonnblad, G. Miu, S. Mrenna and E. Norrbin, Computer Physics Commun. 135 (2001) 238.

$m_{\tilde{t}_1}$ (GeV)	Detection efficiency(%) $e^+e^-$
100	2.0
120	4.6
140	9.2
160	15.0
180	21.8
200	26.7
220	29.8

Table 1: Di-electron plus di-jet detection efficiencies for various  $m_{\tilde{t}_1}$ .

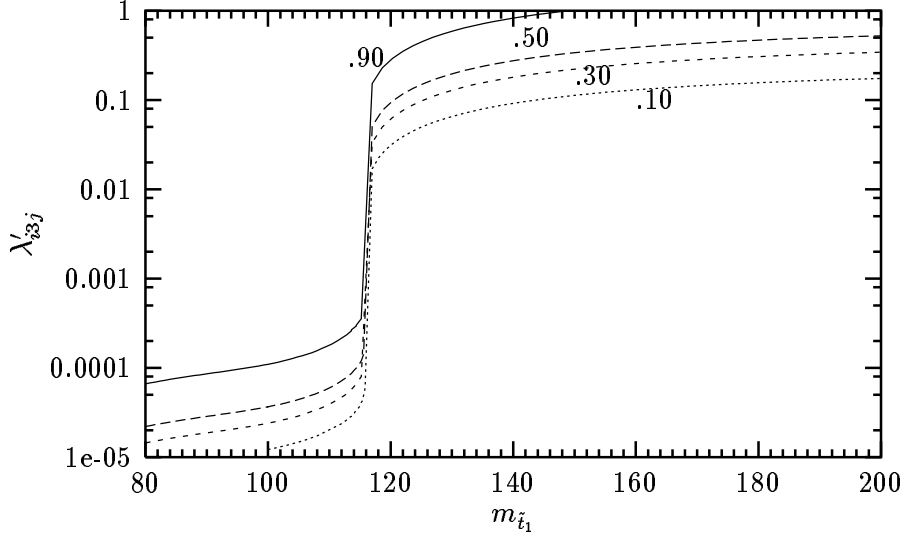


Figure 1: Branching ratio contours for the decay channel  $\tilde{t}_1 \rightarrow \ell + q$ . The SUSY parameters are:  $M_2 = 125$  GeV,  $\mu = 400$  GeV,  $\tan\beta = 4$ ,  $\cos\theta_{\tilde{t}} = 0.8$  and  $m_{\tilde{q}} = 300$  GeV,  $m_{\tilde{\ell}} = 200$  GeV,  $A_b = A_{\tau} = 200$  GeV.

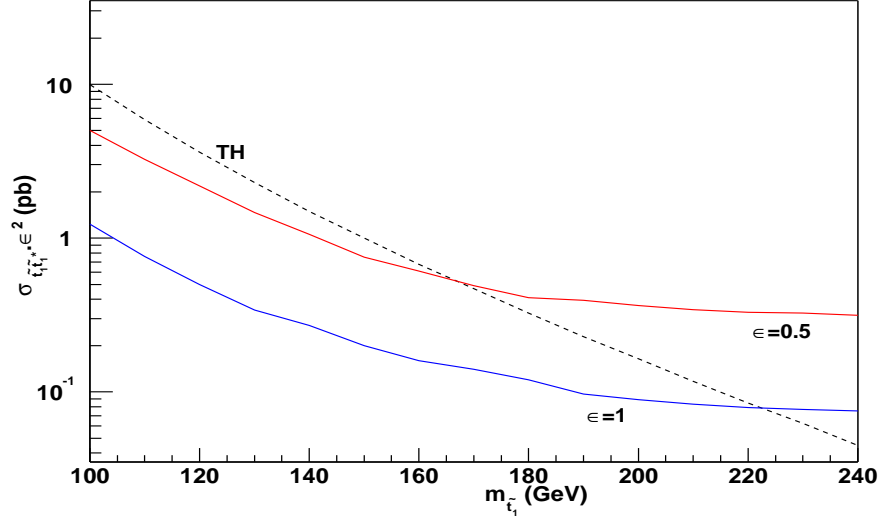


Figure 2: The top squark pair production cross section limits at 95% C.L (solid lines) for  $\epsilon=1$  and 0.5 along with the theoretical prediction(dashed line).

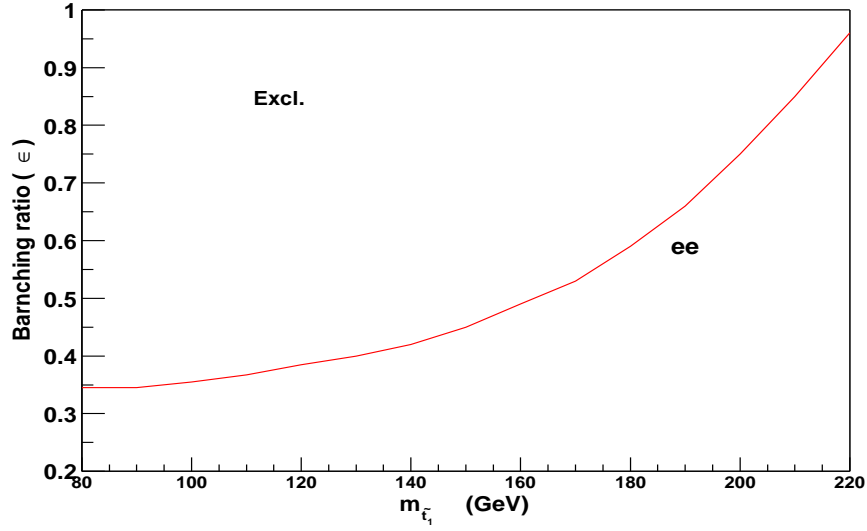


Figure 3: The excluded region by di-electron data at 95% C.L.

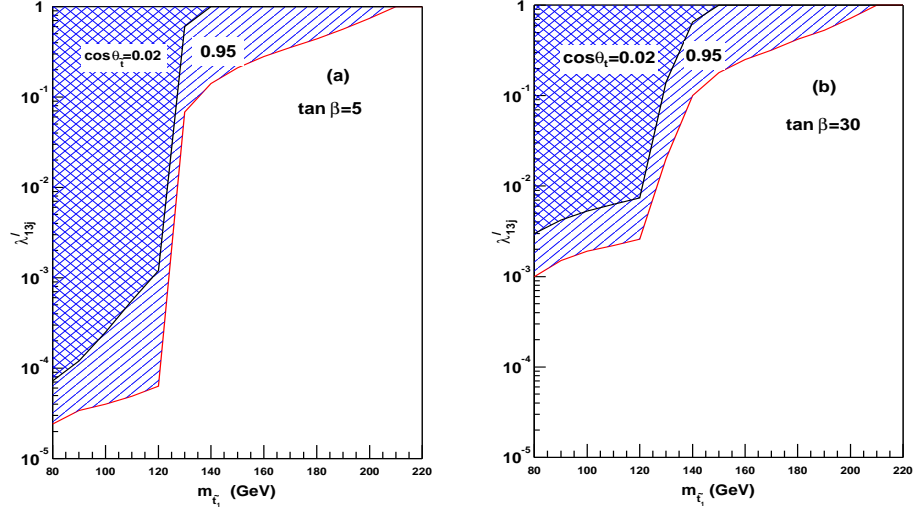


Figure 4: The excluded region(hatched) by di-electron data at 95% C.L. The SUSY parameters are:  $M_2 = 130$  GeV,  $\mu = 500$  GeV,  $m_{\tilde{q}} = 300$  GeV,  $m_{\tilde{\ell}} = 200$  and A-terms=200 GeV.